Effects of Cognitive Distraction on Upper Limb Movement Decoding from EEG Signals

Weijie Fei, *Student Member, IEEE,* Luzheng Bi*, *Senior Member, IEEE*, Jiarong Wang, Shengchao Xia, Xinan Fan, and Cuntai Guan, *Fellow, IEEE*

***Abstract*—Objective: Hand movement decoding from electroencephalograms (EEG) signals is vital to the rehabilitation and assistance of upper limb-impaired patients. Few existing studies on hand movement decoding from EEG signals consider any distractions. However, in practice, patients can be distracted while using the hand movement decoding systems in real life. In this paper, we aim to investigate the effects of cognitive distraction on movement decoding performance. Methods: We first propose a robust decoding method of hand movement directions to cognitive distraction from EEG signals by using the Riemannian Manifold to extract affine invariant features and Gaussian Naive Bayes classifier (named RM-GNBC). Then, we use the experimental and simulated EEG data under conditions without and with distraction to compare the decoding performance of three decoding methods (including the proposed method, tangent space linear discriminant analysis (TSLDA), and baseline method)). Results: The simulation and experimental results show that the Riemannian-based methods (i.e., RM-GNBC and TSLDA) have higher accuracy under the conditions without and with cognitive distraction and smaller decreases in decoding accuracy between the conditions without and with cognitive distraction than the baseline method. Furthermore, the RM-GNBC method has 6% (paired t-test, p=0.026) and 5% (paired t-test, p=0.137) higher accuracies than the TSLDA method under the conditions without and with cognitive distraction, respectively. Conclusion: The results show that the Riemannian-based methods have higher robustness to cognitive distraction. Significance: This work contributes to developing a brain-computer interface (BCI) to improve the rehabilitation and assistance of hand-impaired patients in real life and open an avenue to the studies on the effects of distraction on other BCI paradigms.**

***Index Terms*—EEG; cognitive distraction; hand movement decoding; Riemannian manifold**

I. Introduction

Recently, human-machine collaboration has attracted plenty of research attention from diverse fields, such as human augmentation and rehabilitation [1-4]. In human-machine collaboration, motion intention recognition is one of the most important problems. If motion intention is recognized, the machine is able to actively collaborate with its human partner to improve the performance and safety of the whole system [5-7]. For example, in rehabilitation [8], the rehabilitative devices can actively respond to improve rehabilitation when they can understand patients' motion intentions.

The signals used to recognize motion intention can be classified into nonbiological signals and biological signals. Nonbiological signals include eye gaze, hand position, and head pose. Biological signals mainly contain electromyograms (EMG) and electroencephalograms (EEG) signals. Compared to motion intention recognition methods based on nonbiological signals, those methods based on biological signals may detect people's motion intentions earlier since the biological signals are generated earlier than nonbiological signals. Further, since EEG signals are generated about 200 ms before EMG signals are, motion intention detection methods based on EEG signals may be able to detect motion intention earlier [6].

Many researchers have conducted valuable work regarding human motion recognition (decoding) based on EEG signals. Generally, two kinds of EEG signals, including Sensory Motor Rhythm (SMR) Event-Related Desynchronization / Event-Related Synchronization (ERD/ERS) and movement-related cortical potentials (MRCPs), are used to decode human motion. Compared to ERD/ERS, MRCPs can encode more information (e.g., direction, velocity, and different grasps) and provide intuitive and nature control [9]. Thus, in this paper, we focus on studies on decoding human motion based on MRCPs. In 2008, Waldert *et al*. [10] decoded the hand movement from EEG signals by performing a center-out task and obtained an averaged accuracy of 55% for binary decoding across nine subjects. In 2013, Yeom *et al.* [11] proposed a decoding method that can extract a 3-D trajectory of hand movement from EEG signals and reconstruct hand trajectory with the correlation coefficients of 0.3, 0.3, and 0.15 in x, y, and z axes. In 2015, Jochumsen *et al.* [12] detected movement intention through MRCPs associated with motor executed and imaginary tasks across healthy and stroke participants and showed the possibility of using the single EEG channel in human intention decoding. In 2017, Úbeda *et al.* [13] decoded hand movement direction under the condition between the active and passive movements, which suggested that the

* This work was supported in part by National Natural Science Foundation of China under Grants 51975052 and 51575048. (Corresponding author: Luzheng Bi).

L. Bi, W. Fei, J. Wang, and S. Xia are with the School of Mechanical Engineering, Beijing Institute of Technology, Beijing 100081 China. (e-mail: bhxblz@bit.edu.cn, 3120170241@bit.edu.cn, 18810805389@163.com, shengchaoxia@163.com).

X. Fan, is with the Beijing Machine and Equipment Institute, Beijing, 100854 China. (anmengxiang@126.com).

C. Guan is with the School of Computer Science and Engineering, Nanyang Technological University, Singapore. (ctguan@ntu.edu.sg)

low-frequency EEG signals in movement direction decoding were correlated with the active motion. In 2018, Chouhan *et al*. [14] proposed a wavelet phase-locking value-based (W-PLV) method for decoding hand movement direction and reached a binary classification accuracy of 76.85% across seven subjects. In 2021, Wang *et al.* [15] studied neural signature and decoding of single-hand and both-hand movement directions and obtained a peak accuracy of 70.29% for 6-class classification. These researches show that it is feasible to decode hand motion, especially movement direction, from EEG signals.

Existing studies on decoding hand movement direction do not consider perception, cognitive, or motor distractions, although, in 2020, Fahimi *et al*. [16] considered cognitive distraction when they decoded whether a subject intended to move or not from EEG signals. In practice, distractions are inevitable during the rehabilitation and assistance of people with disabilities. Thus, exploring how to decode hand motion direction given a distraction is valuable.

Researchers have applied Riemannian Manifold to the field of BCIs to enhance their performance. In 2012, Barachant *et al.* [17] used a Riemannian Manifold-based method to develop a motor imagination (MI) BCI. Experimental results showed that the BCI had an accuracy of 70.2% in four-class classification, 5.6% higher than that of traditional methods. In 2017, Wu *et al.* [18] applied Riemannian geometry to develop a method for decoding hand movement trajectories. The Riemannian manifold-based method reduced the estimation root mean square error by 4.30-8.30% and increased the estimation correlation coefficient by 6.59-11.13%. In 2021, Tang *et al.* [19] developed a Riemannian Manifold-based adaptive method for a MI BCI, which extended the Generalized Learning Vector Quantization method in the Euclidean space to the Riemannian space and obtained better performance. These studies show the potential of Riemannian Manifold in enhancing the performance of BCIs. However, no studies apply Riemannian Manifold to decode human movement directions, especially under a condition with a cognitive distraction.

In this paper, we aim at investigating the decoding of hand motion direction under a cognitive distraction and the effects of cognitive distraction on the decoding performance of upper limb movement direction across different decoding methods. Specifically, we use two Riemannian Manifold-based decoding methods. The first method uses the Riemannian Manifold to extract affine invariant features and linear discriminant analysis (named TSLDA), which was proposed in [17]. The second method uses the Riemannian Manifold to extract affine invariant features and Gaussian Naïve Bayes classifier (named RM-GNBC) proposed in this paper. The baseline method is the latest one in decoding hand movement direction (i.e., the W-PLV method proposed in [14]).

The contribution of this paper is that it is the first work to investigate effects of cognitive distraction on motion decoding from EEG signals and show that the Riemannian Manifold-based decoding methods of hand movement direction are more robust to cognitive distraction than the baseline method. The remainder of the paper is organized as follows: Section II introduces the method. Section III presents the results. Section IV describes the conclusion, limitations, and future work.

II. METHOD

A. Participants

Eight participants (aged 20-25 with a mean age of 23) volunteered to participate in the experiment and received no monetary compensation. All participants had no history of brain disease. The study abided by the principles of the 2013 Declaration of Helsinki and was approved by the Beijing Institute of Technology research ethics committee with the approval number of V20211108. All subjects signed the informed consent forms.

B. Experimental Paradigm and Procedure

The experimental procedure included two sub-experiments: 1) a motion task without a cognitive distraction （Sub-experiment 1），and 2) a motion task with a cognitive distraction (Sub-experiment 2). Each sub-experiment included four sessions associated with hand movements in forward, backward, leftward, and rightward directions in the 2-D horizontal plane, respectively. Participants had a 10-min break between every two sessions.

Before the start of the experiment, we explained the experimental procedure to the participants to make them familiar with the experimental protocol. We displayed the interface on a display screen. Each participant was required to sit in a comfortable chair 0.8 meters in front of the screen during the experiment, as shown in Fig. 1. We adjusted the position, size, and intensity of the interface and set the EEG collection system parameters. We placed the electrode cap on the scalp of the subjects correctly. We mapped the rightward and leftward movements of the right hand to the rightward and leftward movements of the cursor with one scaling factor (i.e., 1:1 scaling), respectively. Furthermore, we mapped the forward and backward movements of the right hand to the upward and downward movements of the cursor with one scaling factor (i.e., 1:1 scaling).

In Sub-experiment 1, participants were instructed to move the block in the center of the screen to the destination indicated by their right hands, as shown in Fig. 2 (a). In Sub-experiment 2, participants were required to perform both motion and cognitive tasks. For the cognitive task, the participants were required to perform the *n*-back task, as shown in Fig. 2 (b). The *n*-back task has been widely used to investigate brain structural correlates of working memory and divided attention [20-22]. The 2-back task as a secondary task of the dual-task has shown significant distraction on the attention of the primary task [23-24]. In the 2-back task, an integral number from 0 to 9 was randomly presented by a sound every two seconds. Subjects were instructed to memorize the number presented in the stimuli and recall the number presented 4 seconds ago.

Each session was composed of 50 trials. In each trial, participants were asked to relax before the experimental start. As shown in Fig. 2 (c) (d), at 3 s, the computer beeped, informing participants to get into the idle state. At 6 s, the screen displayed the target position. At that time point, if

participants took Sub-experiment 1, they were asked to keep the idle state; otherwise, they were asked to start to perform the cognitive task. At about 9 s (about 3 s after the target position was presented), participants started to perform the self-paced motion task. At 16 s, the computer beeped again, indicating the end of this trial.

During the whole experiment, participants were asked to fix their eyes on the center of the screen to avoid eye movement interference. Furthermore, they were required not to produce any body movements, which are not related to the experimental requirements.

Fig. 1. Experimental scenario

C. Data Acquisition

The experiment was conducted at the IHMS Lab of the School of Mechanical Engineering, Beijing Institute of Technology, China. EEG signals were collected by a 64-electrode portable wireless EEG amplifier (NeuSen.W64, Neuracle, China) from the scalp of subjects at the Fpz, Fp1, Fp2, AF3, AF4, AF7, AF8, Fz, F1, F2, F3, F4, F5, F6, F7, F8, FCz, FC1, FC2, FC3, FC4, FC5, FC6, FT7, FT8, Cz, C1, C2, C3, C4, C5, C6, T7, T8, CP1, CP2, CP3, CP4, CP5, CP6, TP7, TP8, Pz, P3, P4, P5, P6, P7, P8, POz, PO3, PO4, PO5, PO6, PO7, PO8, Oz, O1, and O2 locations according to an international 10-20 system, with a forehead ground at AFz and reference at CPz. Two extra electrodes E1, E2 were placed behind the two ears. Electro-oculogram (EOG) signals were acquired from two electrodes positioned below and flank the outer canthi of the eyes. The sampling rate was set to be 1000 Hz. Electrode impedances were calibrated to be less than 5 KΩ. The EEG signals from each channel were re-referenced by binaural electrodes E1 and E2.

Furthermore, hand movement trajectories were collected with a motion-tracking device (FASTRAK, Polhemus). The sampling rate was 60 Hz. One tracking sensor was attached to the right hands of subjects.

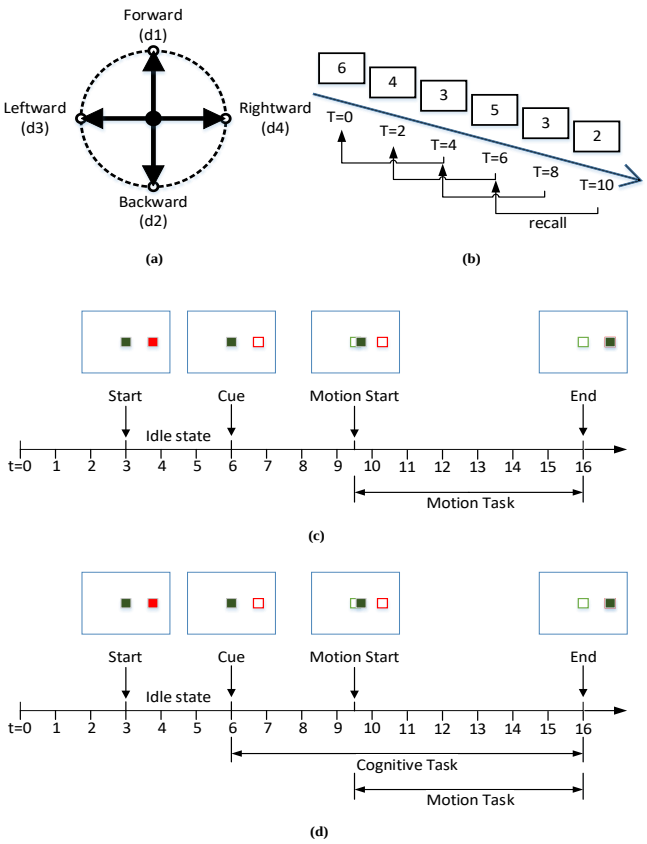

Fig. 2. Experimental paradigm: (a) experimental paradigm for motion task (b) experimental paradigm for cognitive distraction (c) experimental timeline for Sub-experiment 1 (d) experimental timeline for Sub-experiment 2.

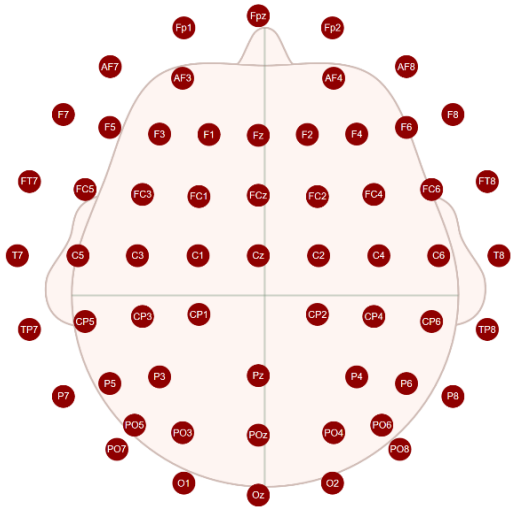

Fig. 3. EEG channels used in this study.

D. Preprocessing

EEG signals were first preprocessed by baseline correction and down-sampled to be 100 Hz [25]. Then, a 0.05-10 Hz band-pass filter was applied. After that, the independent component correlation algorithm (ICA) was used further to remove ocular artifacts [26-27]. The ICA was trained by using data filtered from 2-10 Hz according to the findings in [28]. Note that the trained ICA was applied to data filtered from 0.05-10 Hz to keep the low-frequency EEG signals. Correlation coefficients of independent components (ICs) obtained from EEG signals through ICA and raw time-series EOG signals were computed. The ICs with coefficients larger than 0.6 were generally considered significant correlations [29] and were cleared to remove the ocular artifact. The remaining ICs were inversely transformed for clean EEG data. Furthermore, EEG signals were preprocessed by common average reference (CAR). We applied a Laplacian spatial filter to remove the electromyography (EMG) signals [15], and movement artifacts

were filtered by using artifact subspace reconstruction (ASR) [30].

Hand movement trajectories were resampled to 100 Hz to synchronize EEG and kinematic data. Since the motion task was self-paced, movement onsets were detected by using movement trajectories. Two-dimensional hand movement trajectories were transformed to the distance from the initial position to the current hand position. When the distance was larger than the specific threshold value (preset to be 0.2 cm), the movement was considered to get started, and the onset time was marked. All data processing was done in MATLAB.

We extracted one EEG epoch from -0.5 to 0.5 s with respect to the movement onset in each trial. Therefore, for each session with or without a cognitive distraction, there was a total of 50 epochs (50 trials × one epoch/ trial) for hand motion decoding. That is, 50 samples associated with hand motion without and with the cognitive distraction were obtained, respectively.

Finally, we removed some trials according to the two criteria: (1) trials with maximum absolute amplitude of EEG exceeding 200 μV and (2) trials with abnormal kurtosis (i.e., larger than six standard deviations around the mean over trials). In doing so, the mean with standard deviation of the number of trials removed across all subjects was 6±2 trials.

E. Generative Model of EEG Signals

According to the generative model [31-32], EEG signals can be modelled as a linear combination of sources with additive noise

$$X_i(t) = A_s * S_i(t) + N_i(t) \tag{1}$$

where $X_i(t) \in \mathbb{R}^P$ represents P channels of EEG data measured in the i^{th} epoch in the sensor space, $S_i(t) \in \mathbb{R}^Q$ represents Q source signals of time activity in the i^{th} epoch, $N_i(t) \in \mathbb{R}^P$ refers to the additive noise of all channels, and the matrix $A_s \in \mathbb{R}^{P\times Q}$ represents the Q source patterns.

Suppose that sources are not correlated. The noise $N_i(t) = A_\xi * \xi_i(t)$ is stationary and uncorrelated with the sources ($A_\xi \in \mathbb{R}^{P\times P-Q}, \xi_i(t) \in \mathbb{R}^{P-Q}$). The generative model can be expressed as follows

$$X_i(t) = A * \Phi_i(t) \tag{2}$$

where $A = \begin{bmatrix} A_s & A_\xi \end{bmatrix}$ contains the source and noise patterns and is supposed to be invertible. The vector $\Phi_i(t) = \begin{bmatrix} S_i(t) \\ \xi_i(t) \end{bmatrix}$ includes the source and noise signals.

F. Riemannian Manifold-based Decoding Methods

In this paper, we used *Riemannian Manifold-based Features of EEG* signals, which can be written in the form of a matrix:

$$X_i = \begin{bmatrix} X_t^1 & X_{t+1}^1 & \cdots & X_{t+T-1}^1 \\ X_t^2 & X_{t+1}^2 & \cdots & X_{t+T-1}^2 \\ \vdots & \vdots & \ddots & \vdots \\ X_t^N & X_{t+1}^N & \cdots & X_{t+T-1}^N \end{bmatrix} \tag{3}$$

where X_i corresponds to the i^{th} sample, N is the number of channels, and T denotes the number of sampled time points in each example. Each channel measurement was first regularized with z-score. For the i^{th} example, the spatial covariance matrix was estimated by using the *Sample Covariance Matrix* (SCM) written as

$$P_i = \frac{1}{T-1} X_i * X_i^T \tag{4}$$

The SCM is known to be an unbiased estimator of the covariance matrix provided that the number of observations T is much larger than the number (i.e., N) of variables. Since SCMs are *Symmetric Positive Definite* (SPD) matrices, they belong to the manifold $\mathcal{M}$ [17].

Each SCM P_i is mapped into the tangent space located at the *Riemannian geometric mean* P_G of the whole set of samples [33]. Geometric mean P_G of N SCM matrices $P_i \in \{P_1 \ P_2 \ \cdots \ P_N\}$ is obtained according to [34].

The Riemannian manifold-based features of the i^{th} sample can be described as a $M = N(N+1)/2$ dimensional vector F_i:

$$F_i = lower\left(P_G^{-1/2} * \log_{P_G}(P_i) * P_G^{-1/2}\right) \tag{5}$$

where $\log_{P_G}(.)$ mean the manifold logarithm.

To decrease the feature redundancy and computational cost, we applied the Principal Component Analysis (PCA) to the features to retain 95% main information.

Two classifiers were applied to decode the right-hand movement direction based on Riemannian Manifold features: linear discriminant analysis (LDA) classifier and Gaussian Naïve Bayes (GNB) classifier.

The decoding method based on LDA was called the tangent space linear discriminant analysis (TSLDA) proposed in [17], which can be expressed as

$$Y_i = b_c * F_i + b_0 \tag{6}$$

where $b_c \in \mathbb{R}^{1\times M}$ and $b_0 \in \mathbb{R}$ are parameters of LDA.

The decoding method based on GNB was called *Riemannian Manifold-GNB* proposed in this paper.

The GNB was developed from Naive Bayes Classifier (NBC). NBC methods are a set of supervised learning algorithms based on Bayes' theorem with the "naive" assumption of conditional independence between all features given the value of the class variable [35].

Bayes' theorem states the following relationship, given class variable y and independent features x_1 through x_n:

$$P(y \mid x_1, \ldots, x_n) = \frac{P(y)\, P(x_1, \ldots, x_n \mid y)}{P(x_1, \ldots, x_n)} \tag{7}$$

Using the naive conditional independence assumption that

$$P\left(x_i \left| y, x_1, \ldots, x_{i-1}, x_{i+1}, \ldots, x_n\right.\right) = P\left(x_i \left| y\right.\right) \quad (8)$$

For all x_i, this relationship is simplified to

$$P\left(y \left| x_1, \ldots, x_n\right.\right) = \frac{P(y)\prod_{i=1}^{n} P\left(x_i \left| y\right.\right)}{P\left(x_1, \ldots, x_n\right)} \quad (9)$$

Since $P\left(x_1, \ldots, x_n\right)$ is constant given the input, we can use the following classification rule:

$$P\left(y \left| x_1, \ldots, x_n\right.\right) \propto P(y)\prod_{i=1}^{n} P\left(x_i \left| y\right.\right) \quad (10)$$

$$\hat{y} = \arg\max_{y} P(y)\prod_{i=1}^{n} P\left(x_i \left| y\right.\right) \quad (11)$$

In addition, we can use Maximum A Posteriori (MAP) estimation to estimate $P(y)$ and $P(x_i|y)$. The former is then the relative frequency of Class y in the training set.

GNBC uses the Gaussian Naive Bayes algorithm for classification. The likelihood of the features is assumed to be Gaussian (the proof can be seen in Appendix-C):

$$P\left(x_i \left| y\right.\right) = \frac{1}{\sqrt{2\pi\sigma_y^2}} \exp\left(-\frac{\left(x_i - \mu_y\right)^2}{2\sigma_y^2}\right) \quad (12)$$

The parameters σ_y and μ_y are estimated using maximum likelihood [36]. Mean decoding accuracies were calculated by the 5×5 cross-validation method over all subjects.

G. EEG Sensor Space Model Patterns

The source patterns A_s can be identified according to the algorithm proposed in [32] with the fitted linear model (i.e., (6)). The detailed steps of the algorithm can be found in [32].

Given the trained model parameters (b_c, P_G), the sources pattern A can be identified in the following steps. First, the tangent space pattern d_c associated with b_c is computed.

Next, d_c is inversly transformed to the covariance matrix space to obtain P_d.

Finally, the generalized eigenvalues of P_d and P_G can be calculated.

As the RM-GNBC method is non-linear, the TSLDA method was adopted to identify the EEG sensor space model patterns based on the Riemannian Manifold.

H. Simulation Setting

Since the cognitive distraction may reduce motion-related cortical potentials from related brain regions due to the loss of the mental source to the motion task [37-38], the generative model of EEG signals related to the motion task given the distracted state could be written as

$$X_i(t) = \left(I + \lambda_i\right) A * \Phi_i(t) \quad (13)$$

where $\lambda_i \in \mathbb{R}^{P\times P}$, each parameter of λ_i obeys the distribution $N\left(0, \beta^2\right)$. Larger β may mean larger negative impact of distraction on EEG signals related to the motion task.

The motivation for the model (13) is to generate the simulation data of EEG signals given different levels of cognitive distraction to investigate the effects of different levels of cognitive distraction on movement decoding since the experimental data only reflected a certain level of distraction.

In binary classification problem simulations, we investigated the performance of the three decoding methods as the function of the level of the cognitive distraction. During the simulation, we set three brain sources with two noise sources, and 1000 epochs were generated for testing the performance of decoding methods. First, we generated the pattern matrix A defined as $A = \exp(B)$ with the random matrix $B \sim N(0, 1)$. Second, we introduced the cognitive distraction of the brain sources according to (13). Third, the covariance matrices C_i were generated as follows:

$$\begin{aligned} C_i &= X_i * X_i^T \\ &= \left(A * \Phi_i(t)\right) * \left(A * \Phi_i(t)\right)^T \\ &= A * \Phi_i(t) * \Phi_i^T(t) * A^T \end{aligned} \quad (14)$$

where $\Phi_i(t) * \Phi_i^T(t)$ is linearly correlated with the source signal power, which is set as follows:

$$\Phi_i(t) * \Phi_i^T(t) = \begin{bmatrix} P_{S_i} & 0 \\ 0 & P_{\xi_i} \end{bmatrix} \quad (15)$$

where the random parameter P_{S_i} was evenly evaluated between 0 and 1, and the parameter P_{ξ_i} was generated through $P_{\xi_i} = \xi_i(t) * \xi_i^T(t)$ with $\xi_i(t) \sim N(0, 1)$.

In the simulation, the power of the source P_{S_i} is related to the class of the i[th] epoch. The class label y is generated by using

$$y_i = sign\left(P_{S_i} - \frac{1}{2}\right) \quad (16)$$

Five-fold CV was used to compute the classification accuracies of three decoding methods to evaluate the method performance.

III. RESULTS

A. EEG Source Analysis

Fig. 4 shows the source analysis results of the TSLDA method for a specific subject given the condition with cognitive distraction. As shown in Fig. 4 (a), we found that the TSLDA method primarily depended on the first four sources with the highest four eigenvalues. As shown in Fig. 4 (b), the patterns of sources 1, 2, and 3 had the highest activity in the bilateral sensorimotor and parietal electrodes, whereas the patterns of source 4 had the highest activation in medial prefrontal

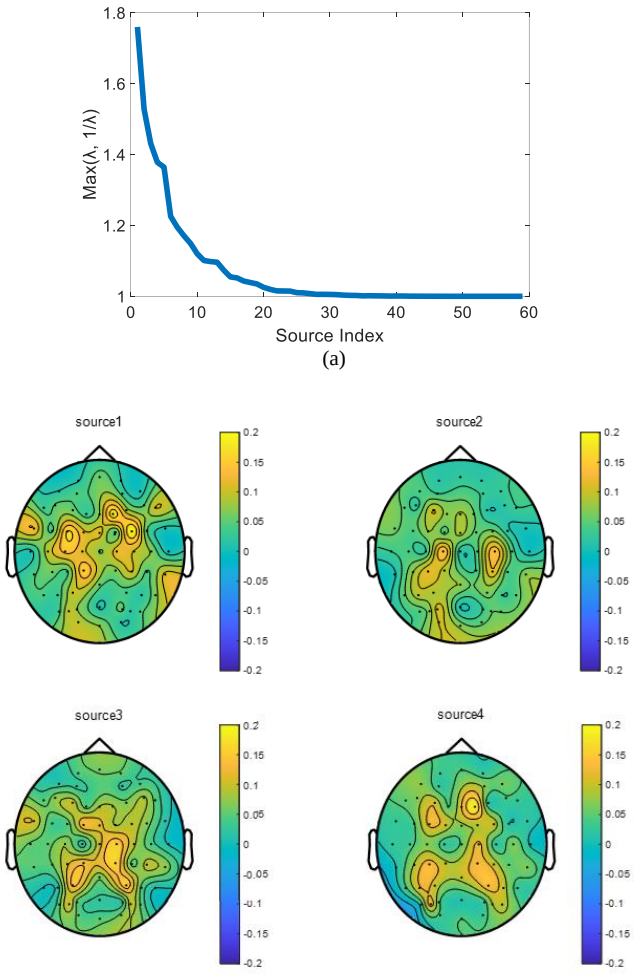

(a)

(b)

Fig. 4 Source analysis results of TSLDA for a specific subject given the cognitive distraction. (a) Eigenvalues (λ) of the TSLDA method with 59 components. The components are ordered in descending order according to max(λ, 1/λ). (b) Patterns of the first 4 Riemann sources.

electrodes. Note that we obtained similar patterns for different CV folds. In addition, although the patterns changed between different conditions and subjects, the patterns of some sources had the highest activity in bilateral sensorimotor and parietal electrodes, while the patterns of some sources had their highest activation in medial prefrontal electrodes for different conditions and subjects.

These results showed that although the Riemannian Manifold-based models relied on the mixture of residual eye artifact and brain activity, they primarily depended on brain activity.

B. Effects of Cognitive Distraction on Decoding Performance of Different Methods

Binary classifications of hand movement directions with and without cognitive distraction were conducted for the two combinations of binary classifications of the four hand-movement directions. For comparison, we implemented the proposed method, W-PLV method in [14], and TSLDA method in [17] and computed the mean accuracies of all methods across the same subjects. The mean accuracies of binary classifications were obtained by the 5 × 5 cross-validation method for all methods. We tested statistical differences between the three methods with the permutation paired t-tests [39-40] and controlled the false discovery rate (FDR) according to [41].

Fig. 5 shows the mean accuracy comparison between the conditions with and without cognitive distraction across the three decoding methods (RM-GNBC, TSLDA, and W-PLV). As shown in Fig. 5, the mean accuracy of the proposed RM-GNBC method slightly decreased from 81% in the situation without cognitive distraction to 78% in the situation with cognitive distraction, and the accuracy decrease of 3% was not statistically significant (paired t-test, p = 0.327 >0.05). The mean accuracy of the TSLDA method in [17] decreased from 75% in the situation without cognitive distraction to 73% in the situation with cognitive distraction, and the accuracy decrease of 2% was not statistically significant (paired t-test, p = 0.128 >0.05). In comparison, the mean accuracy of the W-PLV

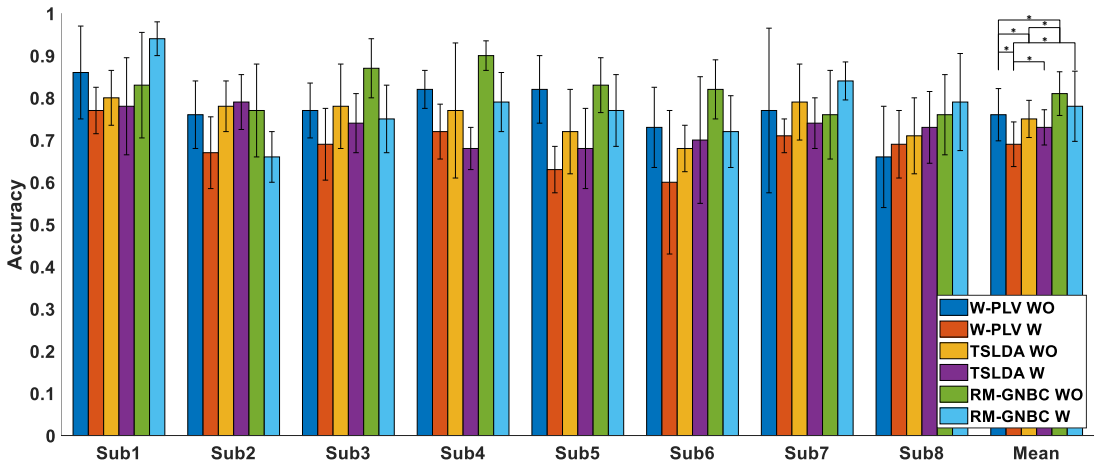

Fig. 5 The performance comparison of three decoding methods between conditions with and without distraction (T-test: $*$ p<0.05). The error bar of each Subject refers to the standard deviation of five CVs. The error bar of the mean result refers to the standard deviation of eight participants.

method significantly decreased by 9% from 77% in the situation without cognitive distraction to 68% in the situation with cognitive distraction (paired t-test, p = 0.005 <0.05). These results suggested that the Riemannian Manifold-based methods (i.e., the RM-GNBC and TSLDA methods) had higher robustness to cognitive distraction than the baseline method (i.e., W-PLV). Furthermore, the proposed method (i.e., RM-GNBC method) showed 6% (81% vs 75%, paired t-test, p=0.026<0.05) and 5% (78% vs 73%, paired t-test, p=0.137 >0.05) higher accuracies than the TSLDA method under the condition without and with cognitive distraction, respectively. More details about decoding accuracy over all subjects can be seen in Appendix-A.

C. Accuracy Comparison of Decoding Methods under Different Levels of Distraction by Simulation

In the simulation, we investigated the performance of three decoding methods given different levels of cognitive distraction. Fig. 6 shows the accuracy comparison results between the three decoding methods given different levels of cognitive distraction. We saw that, if there were almost no cognitive distraction (i.e., the cognitive distraction parameter β in (3) was 0.001), all the three decoding methods performed relatively high accuracy (91.0% for RM-GNBC, 91.3% for TSLDA, and 80.0% for W-PLV). As the cognitive distraction level increased, the accuracy of all decoding methods decreased. However, compared to the W-PLV, the Riemannian Manifold-based decoding methods showed a smaller and smoother accuracy decrease. The simulation results suggested that the Riemannian Manifold-based decoding methods had higher robustness to cognitive distraction than the W-PLV method.

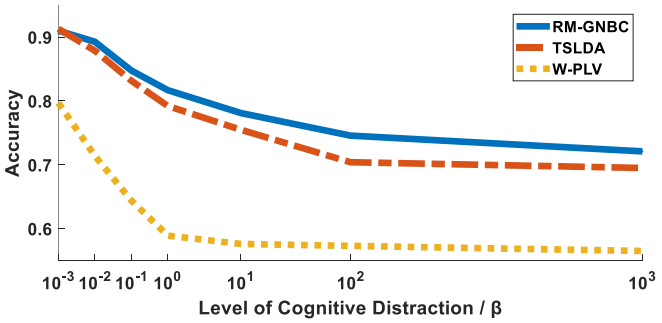

Fig. 6 The performance comparison of three decoding methods under different levels of cognitive distraction in the simulation

IV. Discussion and Conclusion

In this paper, we investigated the decoding of the upper limb movement direction under cognitive distraction by using EEG signals and the effects of cognitive distraction on the decoding performance of upper limb movement direction across the methods based on Riemannian tangent space (including our RM-GNBC and TSLDA in [17]) and the baseline method. The experimental and simulation results suggested that the methods based on Riemannian tangent space were more robust to cognitive distraction than the baseline method, and the RM-GNBC method had 6% (paired t-test, p=0.026) and 5% (paired t-test, p=0.137) higher accuracies than the TSLDA method under the conditions without and with cognitive distraction, respectively.

By comparing the accuracy of these methods between situations without and with cognitive distraction, we found that cognitive distraction degraded the performance of the decoding methods. The accuracy of the baseline method decreased by 9.0%, and the paired t-test showed the accuracy difference was statistically significant (p = 0.005<0.05). In comparison, the accuracy of the proposed RM-GNBC method decreased by 3.0%, and the paired t-test showed that the difference in decoding accuracy was not statistically significant (p =0.327 >0.05). The accuracy of the TSLDA method decreased by 2.0%, and the paired t-test showed that the difference in decoding accuracy was not statistically significant (p =0.128 >0.05). These results suggested that the Riemannian Manifold-based methods (including the proposed and TSLDA methods) had higher robustness to cognitive distraction than the baseline method. The good robustness of the Riemannian Manifold-based methods to cognitive distraction might be owed to the affine invariance of Riemannian Manifold-based features [42].

To further investigate the effects of different levels of cognitive distraction on decoding performance, we built the generative model (13) of EEG signals related to the motion task given the different distraction states and applied this model to generate simulated EEG data under different levels of cognitive distraction. The simulation results showed that when there was almost no cognitive distraction (i.e., the cognitive distraction parameter β in (13) was 0.001), all the three decoding methods performed high accuracy (91.0% for the RM-GNBC, 91.3% for the TSLDA, and 80.0% for the baseline method). As the cognitive distraction level increased, the accuracy of all decoding methods decreased. However, the Riemannian Manifold-based decoding methods (i.e., the RM-GNBC and TSLDA decoding methods) showed a smoother and smaller accuracy decrease than the baseline decoding method. The simulation results suggested that the Riemannian Manifold-based decoding methods had higher robustness to cognitive distraction than the baseline method.

This work contributes to developing a BCI to improve the rehabilitation and assistance of hand-impaired patients and developing active human-centric assistive systems for healthy people in real life. First, the hand-impaired patients may get distracted during rehabilitation and assistance. From this aspect, the Riemannian Manifold-based decoding methods (i.e., the RM-GNBC and TSLDA decoding methods) can have more robust performance and thus may help hand-impaired patients more efficiently. Second, cognitive distraction is common for healthy people. Thus, this work can lay a foundation for the future development of an active human-machine collaboration system based on EEG signals and open a new research direction in the field of decoding hand movement parameters from EEG signals. Furthermore, this work can open an avenue to the studies on effects of cognitive distraction on other BCI paradigms.

Some limits still exist in this paper. First, in this study, we focused on four directions of upper limb movement (i.e.,

moving forward, backward, leftward, and rightward). However, in practice, there are many other hand movement directions. Thus, the proposed method should be further validated for the other hand movement directions (such as moving upward and downward). Second, this work only studied the binary classification of hand motion directions rather than multi-class decoding. Third, we investigated the movement direction decoding from EEG signals with a cognitive distraction. To better apply the proposed method, we should consider more types of distractions, such as visual and auditory distractions. Fourth, as shown in Fig. 4, it may be impossible to completely rule out that the decoding models relied on a mixture of residual eye artifact and brain activity. Fifth, in this paper, the findings on the effects of cognitive distraction on decoding performance are only limited to motor decoding. To generalize the results to other BCI paradigms, we need to perform corresponding experiments and analyses under other BCI paradigms. Sixth, to analyze the effects of different levels of cognitive distraction on decoding performance, we proposed a simple generative model for simulating EEG data given different levels of cognitive distraction according to the current findings [33-34]. However, we did not validate the proposed model. To validate the proposed model, we need to conduct experiments under different levels of cognitive distraction. To perform such experiments, we need to define, generate, and measure different levels of cognitive distraction, which is rather hard, if not infeasible.

APPENDIX A

Detailed Performance of Three Decoding Methods between Conditions with and without Distraction

Tables below showed the detailed results for the three methods given the condition without and with cognitive distractions. In the tables, d1 refers to the forward direction; d2 refers to the backward direction, d3 refers to the leftward direction, d4 refers to the rightward direction.

TABLE I. RESULTS OF BINARY CLASSIFICATIONS USING W-PLV METHOD IN [14] UNDER THE CONDITION WITH AND WITHOUT COGNITIVE DISTRACTION ACROSS ALL SUBJECTS.

	W-PLV									
	without Cognitive Distraction					with Cognitive Distraction				
Subjects	d1-d2	std	d3-d4	std	mean	d1-d2	std	d3-d4	std	mean
Sub1	0.81	0.04	0.82	0.05	0.82	0.75	0.08	0.69	0.05	0.72
Sub2	0.76	0.23	0.78	0.16	0.77	0.63	0.04	0.78	0.04	0.71
Sub3	0.87	0.07	0.85	0.04	0.86	0.73	0.14	0.81	0.08	0.77
Sub4	0.74	0.11	0.58	0.13	0.66	0.71	0.09	0.67	0.07	0.69
Sub5	0.76	0.08	0.77	0.05	0.77	0.73	0.11	0.65	0.06	0.69
Sub6	0.67	0.10	0.78	0.09	0.73	0.67	0.19	0.53	0.15	0.60
Sub7	0.76	0.08	0.75	0.08	0.76	0.68	0.09	0.65	0.08	0.67
Sub8	0.91	0.03	0.73	0.13	0.82	0.72	0.04	0.54	0.07	0.63
mean	0.79	0.09	0.76	0.09	0.77	0.70	0.10	0.66	0.08	0.68
std	0.07	0.06	0.08	0.04	0.06	0.04	0.05	0.09	0.03	0.05

TABLE II. RESULTS OF BINARY CLASSIFICATIONS USING TSLDA METHOD IN [17] UNDER THE CONDITION WITH AND WITHOUT COGNITIVE DISTRACTION ACROSS ALL SUBJECTS.

	TSLDA									
	without Cognitive Distraction					with Cognitive Distraction				
Subjects	d1-d2	std	d3-d4	std	mean	d1-d2	std	d3-d4	std	mean
Sub1	0.77	0.18	0.76	0.14	0.77	0.70	0.07	0.67	0.03	0.68
Sub2	0.73	0.09	0.86	0.09	0.79	0.71	0.04	0.76	0.08	0.74
Sub3	0.79	0.03	0.81	0.10	0.80	0.77	0.07	0.78	0.16	0.78
Sub4	0.76	0.08	0.66	0.10	0.71	0.73	0.08	0.72	0.09	0.73
Sub5	0.78	0.10	0.78	0.10	0.78	0.73	0.07	0.75	0.07	0.74
Sub6	0.75	0.06	0.61	0.05	0.68	0.71	0.10	0.68	0.20	0.70
Sub7	0.82	0.05	0.73	0.07	0.78	0.81	0.08	0.76	0.05	0.79
Sub8	0.79	0.10	0.64	0.10	0.72	0.73	0.09	0.62	0.10	0.68
mean	0.77	0.09	0.73	0.09	0.75	0.74	0.08	0.72	0.10	0.73
std	0.03	0.04	0.08	0.02	0.04	0.03	0.02	0.05	0.05	0.04

TABLE III. RESULTS OF BINARY CLASSIFICATIONS USING OUR PROPOSED RM-GNBC METHOD UNDER THE CONDITION WITH AND WITHOUT COGNITIVE DISTRACTION ACROSS ALL SUBJECTS.

	RM-GNBC									
	without Cognitive Distraction					with Cognitive Distraction				
Subjects	d1-d2	std	d3-d4	std	mean	d1-d2	std	d3-d4	std	mean
Sub1	0.90	0.04	0.89	0.03	0.90	0.79	0.06	0.79	0.08	0.79
Sub2	0.75	0.11	0.76	0.10	0.76	0.78	0.07	0.89	0.02	0.84
Sub3	0.84	0.11	0.82	0.14	0.83	0.93	0.04	0.95	0.04	0.94
Sub4	0.85	0.12	0.66	0.07	0.76	0.75	0.11	0.83	0.12	0.79
Sub5	0.93	0.03	0.81	0.11	0.87	0.73	0.08	0.76	0.08	0.75
Sub6	0.76	0.11	0.87	0.03	0.82	0.71	0.07	0.73	0.10	0.72
Sub7	0.79	0.17	0.75	0.05	0.77	0.68	0.09	0.63	0.03	0.66
Sub8	0.89	0.03	0.76	0.10	0.83	0.77	0.06	0.77	0.11	0.77
mean	0.84	0.09	0.79	0.08	0.81	0.77	0.07	0.79	0.07	0.78
std	0.06	0.05	0.07	0.04	0.05	0.07	0.02	0.09	0.04	0.08

APPENDIX B

Probability Distribution of Riemannian Features

We applied the q-q plots to test the probability distribution of Riemannian features. Fig. 7 shows the q-q plot of one Riemannian feature. The result suggested that the feature can be considered Gaussian. The similar q-q plots of other features were obtained.

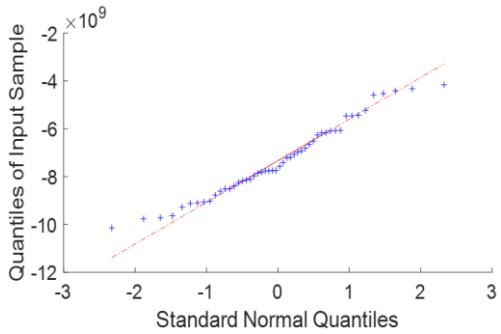

Fig. 7 The q-q plot of one Riemannian feature

REFERENCES

[1]. V. K. Benzy, A. P. Vinod, R. Subasree, S. Alladi and K. Raghavendra, "Motor Imagery Hand Movement Direction Decoding Using Brain Computer Interface to Aid Stroke Recovery and Rehabilitation," in IEEE Transactions on Neural Systems and Rehabilitation Engineering, vol. 28, no. 12, pp. 3051-3062, Dec. 2020.

[2]. R. Foong *et al*., "Assessment of the Efficacy of EEG-Based MI-BCI With Visual Feedback and EEG Correlates of Mental Fatigue for Upper-Limb Stroke Rehabilitation," in IEEE Transactions on Biomedical Engineering, vol. 67, no. 3, pp. 786-795, March 2020.

[3]. K. K. Ang and C. Guan, "EEG-Based Strategies to Detect Motor Imagery for Control and Rehabilitation," in IEEE Transactions on Neural Systems and Rehabilitation Engineering, vol. 25, no. 4, pp. 392-401, April 2017.

[4]. S. Y. Gordleeva *et al*., "Real-Time EEG–EMG Human–Machine Interface-Based Control System for a Lower-Limb Exoskeleton," in IEEE Access, vol. 8, pp. 84070-84081, 2020.

[5]. Z. Li *et al*., "Hybrid Brain/Muscle Signals Powered Wearable Walking Exoskeleton Enhancing Motor Ability in Climbing Stairs Activity," in IEEE Transactions on Medical Robotics and Bionics, vol. 1, no. 4, pp. 218-227, Nov. 2019.

[6]. T. Teng, L. Bi and X. Fan, "Using EEG to recognize emergency situations for brain-controlled vehicles," 2015 IEEE Intelligent Vehicles Symposium (IV), 2015, pp. 1305-1309

[7]. S. Haufe *et al*., "Electrophysiology-baseddetection of emergency braking intention in real-world driving" J. Neural Eng. vol. 11, no. 5,2014.

[8]. A. Pastore *et al*., "Motor intention decoding during the active and robot-assisted reaching," presented at the 7th IEEE International Conference on Biomedical Robotics and Biomechatronics, Enschede, The Netherlands, 2018.

[9]. P. Ofner *et al.* "Attempted Arm and Hand Movements can be Decoded from Low-Frequency EEG from Persons with Spinal Cord Injury," Scientific Reports. vol. 7134, no. 9,2019.

[10]. S. Waldert *et al*., "Hand movement direction decoded from MEG and EEG," Journal of Neuroscience, vol. 28, no. 4, pp. 1000-1008, Jan 23, 2008.

[11]. H. G. Yeom, J. S. Kim, and C. K. Chung, "Estimation of the velocity and trajectory of three-dimensional reaching movements from non-invasive magnetoencephalography signals," Journal of Neural Engineering, vol. 10, no. 2, Apr 2013.

[12]. M. Jochumsen *et al*., "Detecting and classifying movement-related cortical potentials associated with hand movements in healthy subjects and stroke patients from single-electrode, single trial EEG," Journal of Neural Engineering, vol. 12, no. 5, Oct 2015.

[13]. A. Ubeda *et al*., "Classification of upper limb center-out reaching tasks by means of EEG-based continuous decoding techniques," Journal of NeuroEngineering and Rehabilitation, vol. 14, no. 1, p. 9, Feb 1 2017.

[14]. T. Chouhan *et al*., "Wavlet phase-locking based binary classification of hand movement directions from EEG," Journal of Neural Engineering, vol. 15, no. 6, Dec 2018.

[15]. J. Wang, L. Bi, W. Fei and C. Guan, "Decoding Single-Hand and Both-Hand Movement Directions from Noninvasive Neural Signals," in IEEE Transactions on Biomedical Engineering, vol. 68, no. 6, pp. 1932-1940, June 2021.

[16]. F. Fahimi, S. Dosen, K. K. Ang, N. Mrachacz-Kersting and C. Guan, "Generative Adversarial Networks-Based Data Augmentation for Brain-Computer Interface," in IEEE Transactions on Neural Networks and Learning Systems.

[17]. A. Barachant, S. Bonnet, M. Congedo and C. Jutten, "Multiclass Brain–Computer Interface Classification by Riemannian Geometry," in IEEE Transactions on Biomedical Engineering, vol. 59, no. 4, pp. 920-928, April 2012.

[18]. D. Wu, B. J. Lance, V. J. Lawhern, S. Gordon, T. -P. Jung and C. -T. Lin, "EEG-Based User Reaction Time Estimation Using Riemannian Geometry Features," in IEEE Transactions on Neural Systems and Rehabilitation Engineering, vol. 25, no. 11, pp. 2157-2168, Nov. 2017.

[19]. F. Tang, M. Fan and P. Tiňo, "Generalized Learning Riemannian Space Quantization: A Case Study on Riemannian Manifold of SPD Matrices," in IEEE Transactions on Neural Networks and Learning Systems, vol. 32, no. 1, pp. 281-292, Jan. 2021.

[20]. S. Watter, G. M. Geffen and L. B. Geffen, "The n-back as a dual-task: P300 morphology under divided attention". Psychophysiology, 2001, vol. 38, no. 6, pp:998-1003.

[21]. A. M. Owen *et al*. "N-back working memory paradigm: a meta-analysis of normative functional neuroimaging studies," Human Brain Mapping, 2010, vol. 25, no. 1, pp: 46-59.

[22]. S. Lei and M. Roetting, "Influence of task combination on EEG spectrum modulation for driver workload estimation," Human Factors the Journal of the Human Factors & Ergonomics Society, 2011, vol. 53, no. 2, pp: 168-79.

[23]. A. Gevins and M. E. Smith. "Neurophysiological measures of cognitive workload during human-computer interaction," Theoretical Issues in Ergonomics Science, 2003, vol. 4, no. 1, pp: 113-131.

[24]. A. M. Brouwer *et al*. "Estimating workload using EEG spectral power and ERPs in the n-back task," Journal of Neural Engineering, vol. 9, no. 4, 2012.

[25]. J. Omedes, A. Schwarz, L. Montesano and G. Müller-Putz, "Hierarchical decoding of grasping commands from EEG," 2017 39th Annual International Conference of the IEEE Engineering in Medicine and Biology Society (EMBC), Jeju, Korea (South), 2017, pp. 2085-2088.

[26]. T. Teng, L. Bi and Y. Liu, "EEG-Based Detection of Driver Emergency Braking Intention for Brain-Controlled Vehicles," in IEEE Transactions on Intelligent Transportation Systems, vol. 19, no. 6, pp. 1766-1773, June 2018.

[27]. J. T. Gwin, K. Gramann, S. Makeig, and D. P. Ferris, "Removal of movement artifact from high-density EEG recorded during walking and running," Journal of Neural Engineering, vol. 103, no. 6, pp. 3526-34, Jun 2010.

[28]. I. Winkler *et al*., "On the influence of high-pass filtering on ICA-based artifact reduction in EEG-ERP," 2015 37th Annual International Conference of the IEEE Engineering in Medicine and Biology Society (EMBC), 2015, pp. 4101-4105.

[29]. J. Cohen, "The t Test for Means," in *Statistical Power Analysis for the Behavioral Sciences, 2nd ed*. Routledge.1988, pp. 19-74

[30]. N. Robinson, A. P. Vinod, K. K. Ang, K. P. Tee and C. T. Guan, "EEG-Based Classification of Fast and Slow Hand Movements Using Wavelet-CSP Algorithm," in IEEE Transactions on Biomedical Engineering, vol. 60, no. 8, pp. 2123-2132, Aug. 2013

[31]. D. Sabbagh *et al*., "Predictive regression modeling with MEG/EEG: from source power to signals and cognitive states," NeuroImage, vol. 222, 2020.

[32]. R. J. Kobler *et al*., "On the interpretation of linear Riemannian tangent space model parameters in M/EEG," 2021 43rd Annual International Conference of the IEEE Engineering in Medicine & Biology Society (EMBC), 2021, pp. 5909-5913.

[33]. F. Yger, M. Berar and F. Lotte, "Riemannian Approaches in Brain-Computer Interfaces: A Review," in IEEE Transactions on Neural Systems and Rehabilitation Engineering, vol. 25, no. 10, pp. 1753-1762, Oct. 2017.

[34]. H. Karcher, "Riemannian center of mass and mollifier smoothing," Communications on pure and applied mathematics, vol. 30, no. 5, pp. 509–541, 1977.

[35]. A. H. Jahromi and M. Taheri, "A non-parametric mixture of Gaussian naive Bayes classifiers based on local independent features," 2017 Artificial Intelligence and Signal Processing Conference (AISP), 2017, pp. 209-212.

[36]. K. Ryu and R. Myung, "Evaluation of mental workload with a combined measure based on physiological indices during a dual task of tracking and mental arithmetic," Int. J. Ind. Ergon., vol. 35, no. 11, pp. 991-1009, Nov. 2005.

[37]. G. Ying *et al*., "Identification of task parameters from movement-related cortical potentials," Medical & Biological Engineering & Computing, vol. 47, no. 12, pp. 1257-1264, 2009.

[38]. A. P. Dempster, N. M. Laird and D. B. Rubin, "Maximum likelihood from incomplete data via the EM algorithm", J. R. Statist. Soc., vol. 39, no. 1, pp. 1-38, 1977.

[39]. E. Maris, R. Oostenveld, "Nonparametric statistical testing of EEG- and MEG-data," in Journal of Neuroscience Methods, , vol. 164, no. 1, pp. 177-190, 2007.

[40]. T. E. Nichols, A. P. Holmes, "Nonparametric permutation tests for functional neuroimaging: a primer with examples," in Human Brain Mapping, vol. 15, no. 1, pp. 1-25, 2002.

[41]. Y. Benjamini, D. Yekutieli, "The control of the false discovery rate in multiple testing under dependency," in Annals of Statistics, vol. 29, no. 4, 2001.

[42]. P. Zanini, M. Congedo, C. Jutten, S. Said and Y. Berthoumieu, "Transfer Learning: A Riemannian Geometry Framework With Applications to Brain–Computer Interfaces," in IEEE Transactions on Biomedical Engineering, vol. 65, no. 5, pp. 1107-1116, May 2018.